Effects of the surface and interface on the magneto-optical properties in (Co, Ni)/Cu(001) ultrathin films

K. Nakajima*
Department of Applied Physics, Tohoku University, Aoba, Sendai 980-77, Japan

H. Sawada
Joint Research Center for Atom Technology (JRCAT), 1-1-4 Higashi, Tsukuba 305, Japan

T. Katayama
Electrotechnical Laboratory, 1-1-4 Umezono, Tsukuba 305, Japan

T. Miyazaki
Department of Applied Physics, Tohoku University, Aoba, Sendai 980-77, Japan
(Received 28 June 1996; revised manuscript received 30 August 1996)

The thickness dependence of the magneto-optical properties has been investigated for epitaxially grown face-centered-cubic Co and Ni films on a Cu(001) surface. An energy shift toward the low-energy side in the high-energy structure of the off-diagonal conductivity spectra of 20 Å thick films is found for both the Co and Ni films. Non-self-consistent band calculations for the fcc form of Co and Ni are carried out with changing lattice parameter. The calculated conductivity spectra are compared with the experimental results. The energy shift is attributed to the narrowing of the $3d$ band which might be due to the expansion of the atomic volume due to the lattice mismatch in the interface and the reduction of the atomic coordination number in the surface and in the interface. [S0163-1829(96)05846-8]

I. INTRODUCTION

The magneto-optical Kerr effect of artificial multilayers of transition-metal ferromagnets has been one of the major subjects of material research over the last decades, because of its interest for application to recording media. Multilayers of Co, especially, have received much attention because they exhibit a large magneto-optical Kerr effect at shorter wavelengths compared with the materials already made practicable. Numerous experimental studies investigating their magneto-optical properties have been conducted.[1,2] On the other hand, fundamental research in a different direction, including quantum size effect,[3] nonequilibrium phases such as face-centered-cubic Co,[4] crystallographic orientation dependence of the Kerr effect,[5] and granular structure,[6] have been carried out recently. These studies have attracted our attention again to the usefulness of magneto-optical Kerr effect spectroscopy as an experimental technique for investigating the electronic structure of ferromagnets.

In ferromagnets, with the presence of both the ferromagnetic exchange splitting and the spin-orbit coupling, the conductivity tensor is not diagonal, and magneto-optical Kerr effects are produced. The conductivity tensor is an important physical quantity for the study of the electronic structure of metals. For bulk Fe, Co, and Ni, spectra of the off-diagonal elements of the conductivity tensor covering the photon energy range of 1 to 6 eV have been reported by Krinchik and Artemiev,[7] Erskine and Stern,[8] and Buschow.[9] From their results, in the above photon energy range, the spectrum of the absorptive part of the off-diagonal conductivity tensor (Im $\omega\sigma_{xy}$) of Fe, Co, and Ni has roughly two features. One is a high positive peak located at about 1.5 eV, and the other is a zigzag structure at around 5.5 eV. Im $\omega\sigma_{xy}$ changes its sign from positive to negative in the vicinity of 5.5 eV. Theoretical investigations on Fe, Co, and Ni pointed out that interband transitions in both spin bands were responsible for the high-energy structure.[10–13] The transitions occur between the hybridized s-d bands located bottom of $3d$ band (1 band) and the higher p-like bands above the Fermi level (6 band). Those are permitted along the Σ axis and in the vicinity of the symmetry points X and L. It is considered that the zero-crossing point of the Im $\omega\sigma_{xy}$ spectrum is approximately proportional to the $3d$-band width.[8,13]

The $3d$-band width depends strongly on the lattice spacing, as well as on the atomic coordination number. In ultrathin films, it is generally believed that the reduction of the coordination number in the surface will result in a narrowing of the $3d$ bands. In addition, a larger lattice parameter due to the lattice mismatch in the interface will causes a narrowing of the $3d$ bands. In theoretical investigations, the shift of the high-energy structure of the Kerr spectra with changing the lattice parameter has been mentioned by Oppeneer *et al.*[14] Recently, Gasche, Brooks, and Johansson[15] performed a similar investigation for the case of fcc Co. Gasche observed that an increase of the lattice parameter by 6% leads to approximately an 1 eV shift of the high-energy zero-crossing point in the Kerr rotation spectra. Relatively few experimental studies, however, have been carried out to study this problem. In the previous paper,[16] we reported that the high-energy structure in the Im $\omega\sigma_{xy}$ spectrum of a 20 Å thick fcc Co film grown on a Cu(001) surface was clearly different from that of a 1000 Å thick film. The spectrum of the 20 Å thick film changed its sign from positive to negative at around 5 eV, but the spectrum of the 1000 Å thick film was

still positive at 5 eV. Assuming a narrowing of the $3d$ bands for 20 Å thick films, we are able to understand our results on the basis of these theoretical investigations.

To obtain a better understanding of the unique magneto-optical properties of the ultrathin films, we performed a systematic study of the magneto-optical Kerr effects of fcc Co(001) and Ni(001) ultrathin films grown on Cu(001) surfaces. In our discussion, we will compare the experimentally obtained conductivity spectra with those evaluated from non-self-consistent band calculations including lattice distortions. This will be used to provide significant information about the modified electronic structure of the ultrathin films.

II. EXPERIMENTAL

Both 20 and 1000 Å thick Co and Ni films were prepared by means of electron-beam heating in a chamber with a base pressure less than 5×10^{-11} Torr. A polished MgO single crystal was used as a substrate. Prior to the deposition, the MgO substrate was heated to 830 °C in order to remove adsorbed gases. First, an Ag buffer layer of 1000 Å thick was deposited at room temperature to alleviate the lattice mismatch between Cu and MgO. On top of the Ag buffer layer, a Cu seed layer was deposited. We chose a thickness of this seed layer of 2000 Å in order to avoid light transmission and/or interference effects. The Co or Ni layer was grown on this seed layer at room temperature. The growth rate of Co and Ni was 2 Å/min. The thickness of the layers and the growth rate were measured by means of a calibrated quartz thickness monitor. The calibration was performed with an accuracy of 10% using the intensity oscillations associated with reflection high-energy electron diffraction (RHEED).[16] Growth mode and crystal structure were monitored during the deposition by using a RHEED apparatus and a digital camera system.

Ellipsometric measurements were performed using an *in situ* spectrometer in a background pressure of 1×10^{-9} Torr. Details of the apparatus have been reported previously.[17] The angle of incidence was set at 55.7° from the surface normal. The complex Kerr rotation $\theta_k+i\eta_k$ was measured using the Faraday-cell modulation method[17,18] in both the polar and the longitudinal configuration. The complex optical parameter $n+ik$ was measured by the rotating analyzer method.[19] The spectra were measured in the photon energy range 1.7 to 5.1 eV in a remanent state in order to reduce the Faraday effect associated with the vacuum windows. Hysteresis curves were determined by measuring the Kerr rotation angle as a function of the applied field of up to 2.3 kOe.

For 1000 Å thick films, in order to study the high-energy structure of the Kerr spectra above 5.1 eV, we also performed *ex situ* Kerr effect measurements with an improved JASCO-2500 spectrometer. This spectrometer is based on the piezobirefringent modulation method.[20] The angle of incidence was set at 10°. The *ex situ* measurements were done in the photon energy range of 1.7 to 6.0 eV in the polar configuration with a magnetic field of 18.8 kOe. All experiments were carried out at room temperature. No protection layers for oxidation were employed.

III. EXPERIMENTAL RESULTS

RHEED patterns observed during the growth of 1000 Å thick films essentially maintained the same fourfold symmetry as that of the Cu(001) surface. Conventional x-ray-diffraction patterns for a 1000 Å thick Co and Ni film are shown in Fig. 1 together with that of a 2000 Å thick Cu film. In the insets of the figure are enlarged figures around 50°. Only a fcc (002) peak are found in both cases. An interlayer spacing of the peak is 1.770 and 1.755 Å for Co and Ni, respectively. The former is in good agreement with the (002) spacing found for thick fcc Co films ($d=1.772$ Å).[21] Figure 2(a) shows thickness dependence of the lateral lattice parameter for fcc Co, which was measured by means of *in situ* RHEED observation during the film growth. The lattice parameter were evaluated from intervals between (01) and (01) streaks in RHEED images along the [100] direction. The accuracy of the measurements is ±0.01 Å. The lateral lattice parameter for the 20 Å thick layer takes a value of 3.59 Å which is about 0.6% less than that for the Cu substrate and is also about 1.4% expanded from that of the 1000 Å thick fcc Co film. The lattice parameter approaches that of the bulk fcc Co film asymptotically with thickness. In the case of fcc Ni, a similar change of the lattice parameter can be seen in Fig. 2(b). The lateral lattice parameter of the 20 Å thick film is 3.59 Å. This is about 2.0% expanded from that of the intrinsic value for bulk fcc Ni. The result for Ni is consistent with that reported by Matthews and Crawford.[22]

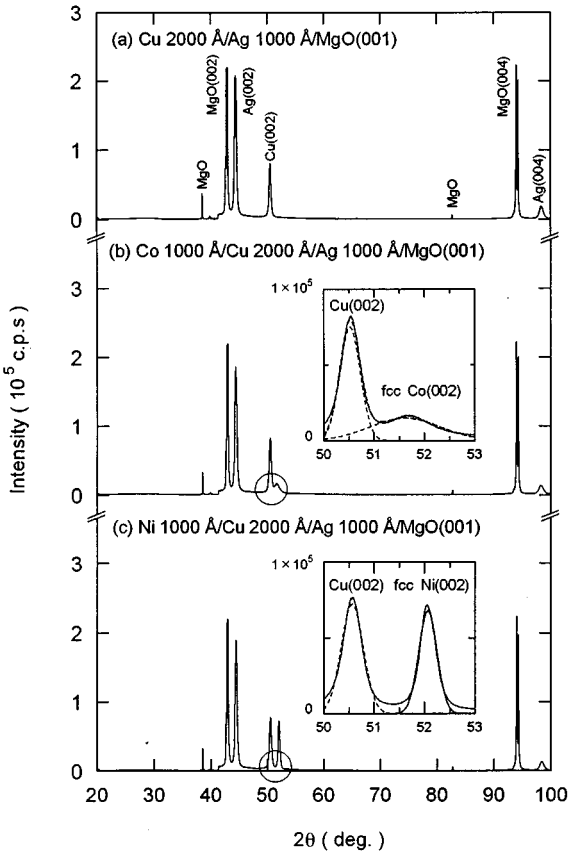

FIG. 1. X-ray-diffraction patterns for 1000 Å thick Co and Ni films grown on Cu 2000 Å/Ag 1000 Å/MgO(001) substrates. Insets are enlarged figures around 50°.

Chappert and Bruno[23] presented a phenomenological model for the relaxation process due to lattice-mismatch-induced strain. They assumed that the lateral strain ε can be written as

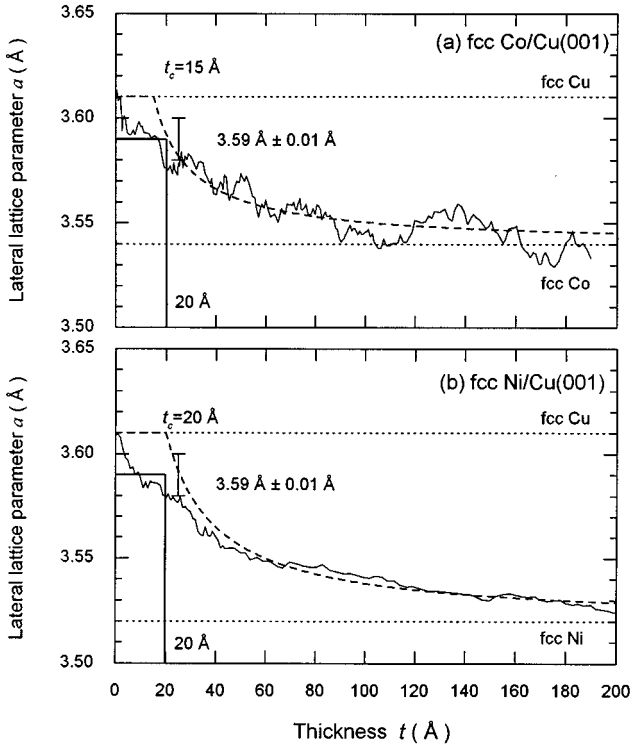

FIG. 2. Lateral lattice parameter a of (a) fcc Co and (b) fcc Ni film grown on a Cu(001) surface as a function of the film thickness t. The lattice parameter were measured by means of *in situ* RHEED observation. The dashed lines show calculated values using Eq. (1). We assumed the lattice parameter for bulk fcc Co is 3.54 Å, that for bulk Ni is 3.52 Å, and that for Cu is 3.61 Å.

$$\varepsilon = \eta \frac{t_c}{t}, \tag{1}$$

where t is thickness of the layer, t_c is critical thickness above where dislocations begin to appear and η is the lattice mismatch. In Figs. 2(a) and 2(b), we have displayed the dependence calculated from Eq. (1) by broken curves with $t_c = 15$ and 20 Å for the fcc Co and the fcc Ni, respectively. We can see that the thickness dependence of the lateral lattice parameter can be explained well by their model.

Before the spectroscopic measurements, *in situ* Kerr hysteresis measurements during the growth of the 20 Å thick films were carried out at a fixed wavelength of 500 nm. For Co, the Kerr loop was observed first at 6 Å with an in-plane easy axis. The magnetization was observed to lie in-plane for thickness up to 20 Å. By contrast, for Ni, the polar Kerr loop with the remanence ratio of unity was observed above 13 Å. These behaviors agree with previous results.[24–26] Though a predominant in-plane magnetization was reported for the samples below 13 Å by Wu *et al.*[27] and O'Brien and Tonner[28] we did not observe both an inplane component and a perpendicular component of the magnetization. The typical coercivity of the 20 Å thick films were 250 Oe for Co and 300 Oe for Ni. For the 1000 Å thick films, an in-plane easy axis was observed in both cases.

The polar Kerr rotation and ellipticity spectra for the 1000 Å thick fcc Co(001) film are shown in Fig. 3(a). These spectra were measured *ex situ* with a magnetic field of 18.8 kOe.

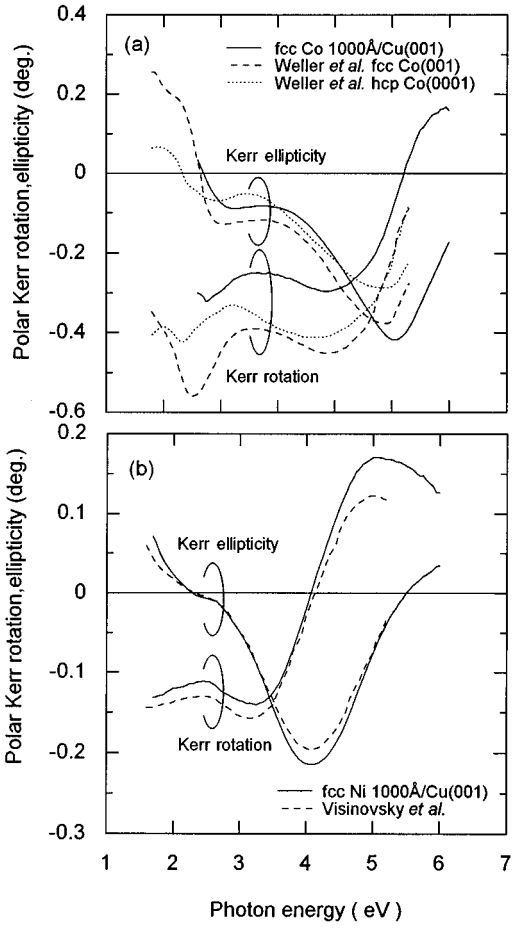

FIG. 3. Polar Kerr spectra for fcc Co and Ni 1000 Å/Cu(001) compared with the experimental data of Weller *et al.* (Ref. 5) and Visinovsky *et al.* (Ref. 29). Our spectra were measured *ex situ* with a magnetic field of 18.8 kOe.

Also shown are the data of single-crystal fcc Co(001) and hcp Co(0001) films reported by Weller *et al.*[5] Our data are similar to those of fcc Co(001) and slightly different from hcp Co(001) at the low-energy side. The magnitude of the Kerr rotation angle and ellipticity, however, are smaller than those of Weller's data by 0.05°–0.2°. This may be due the difference of the intensity of applied field. Figure 3(b) shows the polar Kerr rotation and ellipticity spectra for the 1000 Å thick fcc Ni(001) film. These spectra are in good agreement with those presented by Visnovsky *et al.*[29]

Figures 4(a) and 4(b) show the σ_{xx} and $\omega\sigma_{xy}$ spectra for fcc Co. Also shown are the σ_{xx} spectra of polycrystalline Co film reported by Johnson and Cristy.[30] The diagonal and off-diagonal elements of the conductivity tensor of the film, σ_{xx} and $\omega\sigma_{xy}$, were calculated from the measured value of the complex Kerr rotation $\theta_k + i\eta_k$ and the complex optical parameter $n + ik$. We assume here a time dependence of the electric field as $e^{-i\omega t}$, and hence we specify the diagonal and off-diagonal elements of the conductivity tensor as $\sigma_{xx} = \sigma'_{xx} + i\sigma''_{xx}$ and $\omega\sigma_{xy} = \omega\sigma'_{xy} + i\omega\sigma''_{xy}$, respectively. In the low-energy range below 3 eV, both of our spectra show good agreement in shape. However, there is a noticeable difference between the $\omega\sigma_{xy}$ spectra for the 20 Å thick film and for the 1000 Å thick film above 3 eV. For the 1000 Å thick film,

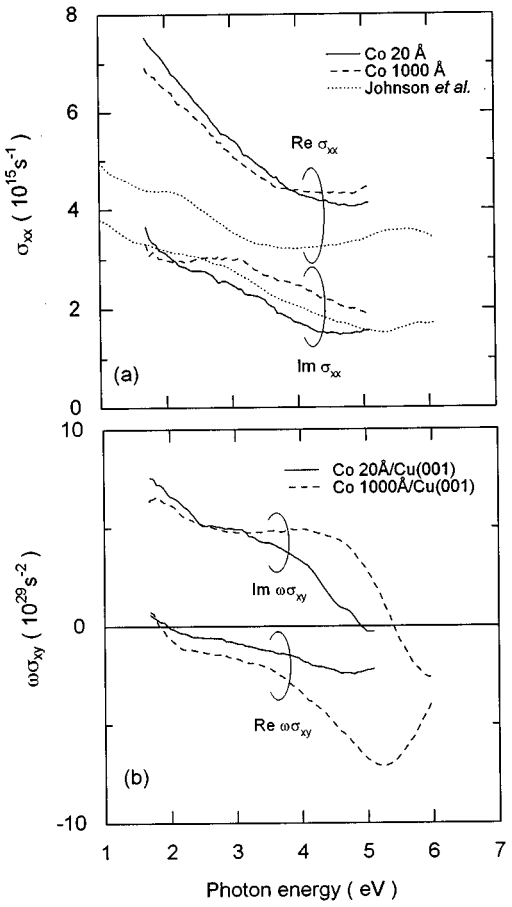

FIG. 4. Diagonal and off-diagonal conductivity spectra of fcc Co/Cu(001) films. The solid and broken curves correspond to 20 and 1000 Å thick films, respectively. The off-diagonal conductivity of 20 Å thick film were calculated from the longitudinal Kerr spectra measured *in situ*. The 1000 Å data were calculated from the polar Kerr spectra measured *ex situ* with a magnetic field of 18.8 kOe. The dotted curves are data of Johnson and Cristy (Ref. 30).

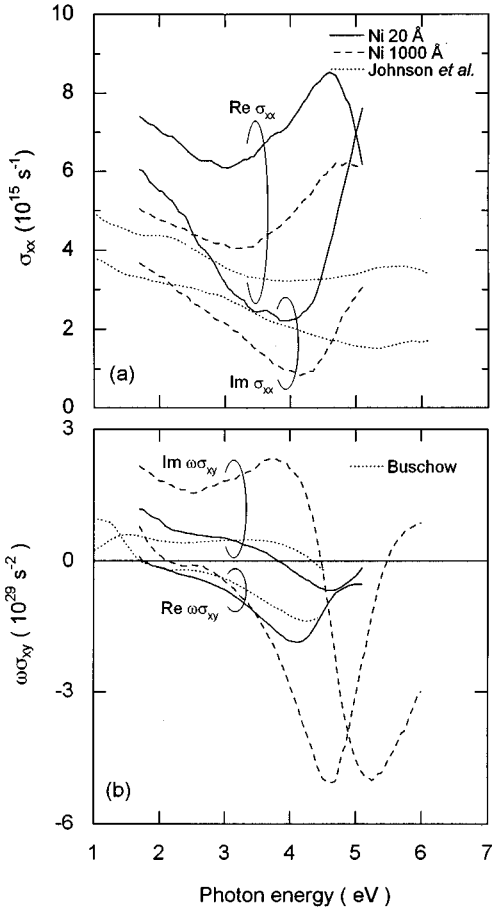

FIG. 5. Diagonal and off-diagonal conductivity spectra of fcc Ni/Cu(001) films. The solid and broken curves correspond to 20 and 1000 Å thick films, respectively. The off-diagonal conductivity of 20 Å thick film were calculated from the longitudinal Kerr spectra measured *in situ*. The 1000 Å data were calculated from the polar Kerr spectra measured *ex situ* with a magnetic field of 18.8 kOe. The dotted curves and the dash-dotted curves are data of Johnson and Cristy (Ref. 30) and Buschow (Ref. 9), respectively.

the $\omega\sigma_{xy}$ spectra exhibit a resonance-type structure at around 5.4 eV. The Re $\omega\sigma_{xy}$ spectrum has a negative broad peak at 5.3 eV. The Im $\omega\sigma_{xy}$ spectrum is correspondingly dispersive and changes its sign at around 5.4 eV. However, the $\omega\sigma_{xy}$ spectra for the 20 Å thick film exhibits a similar resonance structure but at a lower the energy. The Im $\omega\sigma_{xy}$ spectrum crosses zero at 4.9 eV which is 0.5 eV lower than that of the 1000 Å thick film. It is of interest that no clear differences are observed between the σ_{xx} spectra for the 20 Å thick film and for the 1000 Å thick film.

Figures 5(a) and 5(b) show the σ_{xx} and $\omega\sigma_{xy}$ spectra for fcc Ni. For comparison, the σ_{xx} spectra of polycrystalline Ni film reported by Johnson and Cristy[30] and the $\omega\sigma_{xy}$ spectra of bulk fcc Ni reported by Buschow[9] are shown. Apparently, the high-energy structure of the $\omega\sigma_{xy}$ spectra of the 20 Å thick film shifts to the lower energy side, while the shape of the low-energy structure does not change much. The zero-crossing point of the Im $\omega\sigma_{xy}$ spectrum for the 20 Å thick film is 3.8 eV which is 0.6 eV lower than that of the 1000 Å thick film. The σ_{xx} spectra for the 20 Å thick film and for the 1000 Å thick film are alike in shape. This behavior bears a striking resemblance to that observed in the fcc Co film.

IV. NUMERICAL RESULTS AND COMPARISON WITH EXPERIMENT

The interpolation scheme has been used here to construct the electronic structure and evaluate the conductivity spectra of bulk fcc Co and Ni. The scheme is roughly the same as the one described by Smith and Mattheiss.[31] We used a 9×9 Hamiltonian involving four orthogonalized plane waves in addition to five d-type basis functions in terms of linear combination of atomic orbitals given by Slater and Koster.[32] A 5×5 secular equation for d-d block is described using three two-center overlap parameters V_{ddm} $(m=\sigma,\pi,\delta)$. We introduce a following parametized relation between the two-center overlap parameters V_{ddm} and the lattice parameter a:

$$V_{ddm}=\eta_{ddm}\, a^{-5}. \tag{2}$$

The coefficients η_{ddm} and other parameters using to describe a 4×4 conduction block and a 5×4 hybridization block were determined by fitting energies of several sets of high symmetry points Γ, X, L, and W to the results of first-principles calculations. We used a calculation based on the local spin-

density approximation for bulk fcc Co ($a=3.540$ Å). Also used is a calculation of Wang and Callaway[33] for bulk fcc Ni ($a=3.516$ Å). The exchange splitting was included by shifting the diagonal matrix elements of the minority-spin upward relative to those for the majority-spin.

Spectra of the absorptive parts of the diagonal and off-diagonal conductivity tensor, i.e., Re σ_{xx} and Im $\omega\sigma_{xy}$ have been calculated over the photon energy range of 0.5 to 8 eV. Only contributions from the interband transition were taken into account. In the limit of infinite relaxation time, the real part of diagonal elements of the conductivity tensor becomes[33]

$$\mathrm{Re}\sigma_{xx}=\frac{e^2\pi}{m^2\hbar}\sum_{\lambda\neq\lambda}\int dk^3\,\frac{1}{\omega_{mn}}\,|p_x^{\lambda\lambda'}(\mathbf{k})|^2\delta(\omega-\omega_{mn}), \tag{3}$$

and the imaginary part of the off-diagonal elements is[33]

$$\mathrm{Im}\ \omega\sigma_{xy}=\frac{e^2\pi}{m^2\hbar}\sum_{\lambda\neq\lambda}\int dk^3\,\frac{1}{\omega_{mn}}\,\mathrm{Im}(p_x^{\lambda\lambda'}(\mathbf{k})p_y^{\lambda\lambda'}(\mathbf{k}))\times\delta(\omega-\omega_{mn}), \tag{4}$$

where ω_{mn} is an energy difference between final and initial bands m, n. $p_x^{\lambda\lambda'}(\mathbf{k})$ and $p_y^{\lambda\lambda'}(\mathbf{k})$ are x,y components of the matrix element of the momentum operator $\mathbf{p}$ at the wave vector $\mathbf{k}$. For Bloch states, the Cartesian components of the matrix element p_i $(i=x,y)$ is approximately given by[34]

$$p_i^{\lambda\lambda'}(\mathbf{k})=\frac{m}{\hbar}\frac{\partial H^{\lambda\lambda'}(\mathbf{k})}{\partial k_i}, \tag{5}$$

where $H^{\lambda\lambda'}$ is $\lambda\lambda'$ component of the Hamiltonian H.

Inclusion of the spin-orbit interaction is indispensable to evaluate the off-diagonal elements of the conductivity tensor. To simplify the problem, we considered the spin-orbit effect as a first-order perturbation on the Hamiltonian H, because the spin-orbit effect would produce a small change on the band energy in the same degree as the accuracy of the computation. Following Argyres[35] and Cooper,[36] Eq. (4) may be written,

$$\mathrm{Im}\ \omega\sigma_{xy}=\pm A\,\frac{e^2\pi}{m^2\hbar}\sum_{\lambda\neq\lambda}\int dk^3\,\frac{1}{\omega_{mn}}\,p_x^{\lambda\lambda'}(\mathbf{k})\times p_y^{\lambda\lambda'}(\mathbf{k})\,\delta(\omega-\omega_{mn}), \tag{6}$$

where the plus sign is for majority spin and the minus sign for minority spin, A is the one-electron spin-orbit parameter for free atoms, and $p_x^{\lambda\lambda'}(\mathbf{k})$ and $p_y^{\lambda\lambda'}(\mathbf{k})$ are then the matrix elements of the momentum operator $\mathbf{p}$ without the spin-orbit interaction terms. The spin-orbit parameter A is not an adjustable parameter, hence we treated A as a given parameter and did not consider absolute values of the conductivity tensor.

In Figs. 6 and 7, we displayed the calculated conductivity spectra for bulk fcc Co and Ni. We used here the experimental values of $a=3.54$ and 3.52 Å for the lattice parameters of Co and Ni, respectively. In the calculation, the lifetime effect was not taken into account. Results of the different computations by Halilov and Uspenski,[13] Oppeneer *et al.*,[37] and

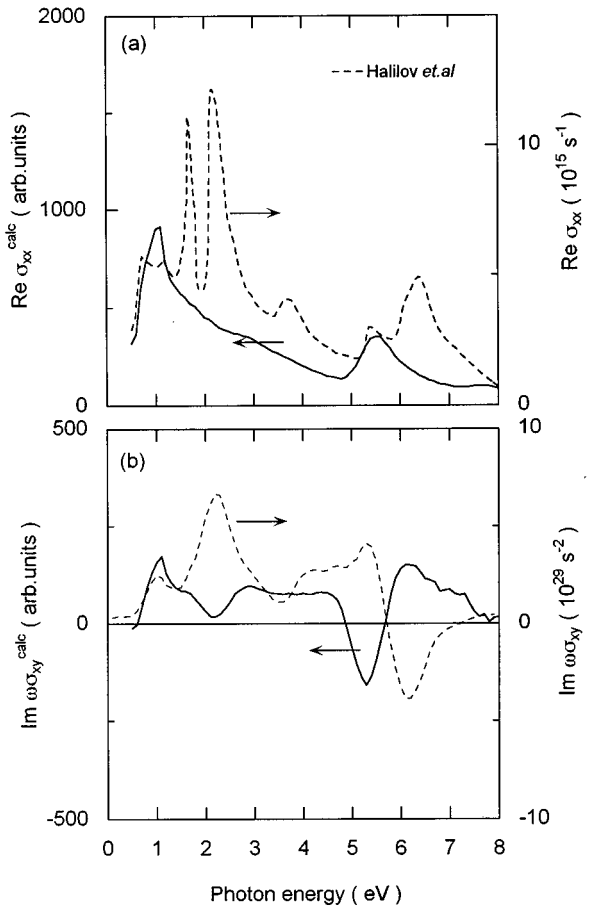

FIG. 6. Calculated conductivity spectra for fcc Co. Solid curves: present work, broken curves: Halilov and Uspenski (Ref. 13).

Wang and Callaway[33] are also shown in the figures. Although our calculation are not self-consistent, for the diagonal conductivity Re σ_{xx}, the features of the spectra bear a strong resemblance to those three calculations. In the case of the off-diagonal conductivity Im $\omega\sigma_{xy}$, the comparisons are much less satisfying than that for the diagonal conductivity. Our calculations reproduce the clear structure above 4 eV, where the spectrum switches sign from positive to negative, but the locations are shifted to the lower energy side compared with all other calculations, for both Co and Ni. This might be due to the inadequacy of our use of the basis functions to represent s, p-like states.

Figures 8(a) and 8(b) show the calculated Re σ_{xx}, Im $\omega\sigma_{xy}$ spectra for fcc Co, respectively. We have calculated the spectra for the lattice parameter changed by ±2 and ±5 % with respect to the experimental value. For the Im $\omega\sigma_{xy}$ spectrum, the high-energy structure is clearly seen to shift with changing lattice parameter. It should be noted that the zero-crossing point in the structure shifts to the lower energy side with increasing lattice parameter. The shift of the zero-crossing point is about 0.5 eV for a 5% increase in lattice parameter. The decrease of the lattice parameter leads to an increase in the zero-crossing point. The low-energy structure of the Im $\omega\sigma_{xy}$ spectra are, however, stable with changing lattice parameter. By considering the corresponding band structures, it turned out that the position of the lower hybridized s-d bands (1 band) near X_1^l and L_1^l were conspicuously moved up and down by changing the

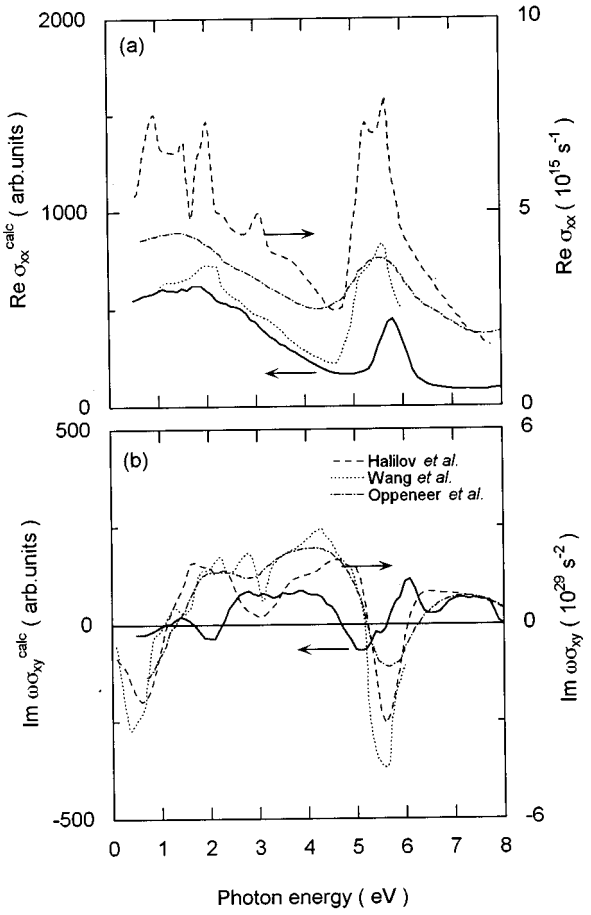

FIG. 7. Calculated conductivity spectra for fcc Ni. Solid curves: present work, broken curves: Halilov and Uspenski (Ref. 13), dotted curves: Wang and Callaway (Ref. 33), dashed-dotted curves: Oppeneer *et al.* (Ref. 37).

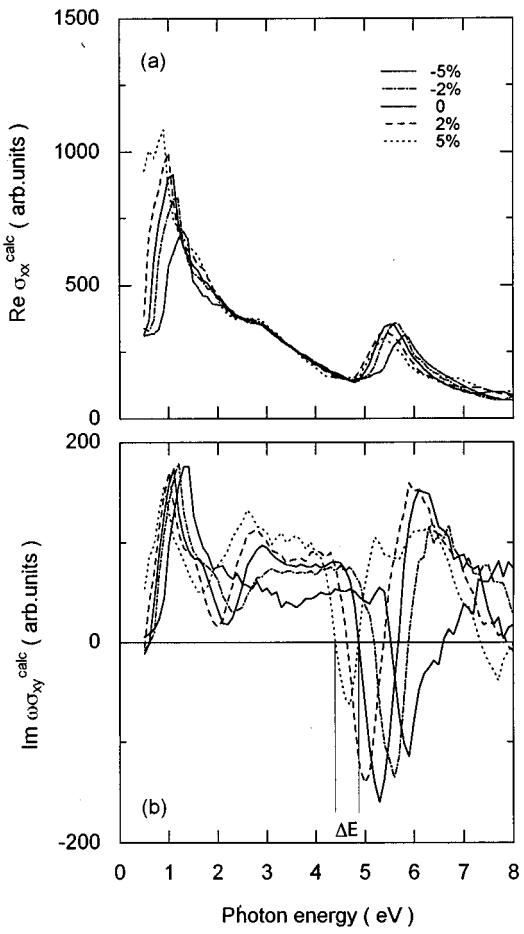

FIG. 8. Calculated conductivity spectra for fcc Co as a function of the lattice parameter.

lattice parameter. The bands close to the Fermi energy, however, do not change much. Therefore, the shift of the 1 band, namely the narrowing of the $3d$-band width, may account for the change in the high-energy structure in the Im $\omega\sigma_{xy}$ spectrum. A point to which special attention should be paid is that the structure of the Re σ_{xx} spectrum is seen to remain unchanged in the entire photon energy range. Apparently, this behavior is also true for the case when we compare the experimental conductivity spectra of the 20 Å thick fcc Co film with those for the 1000 Å thick film (see Fig. 4). Band-by-band decomposition of the conductivity spectra indicate that the transition along the Σ axis is primarily responsible for the high-energy structure in the Re σ_{xx} spectrum, while the transition in the vicinity of the X and L points is responsible for the Im $\omega\sigma_{xy}$ spectrum. This assignment is identical with that of Smith, Lasser, and Chiang.[11] Hence, the discrepancy in the behavior between the Re σ_{xx} and the Im $\omega\sigma_{xy}$ spectrum is mainly due to the difference in location of the transition which contributes to the high-energy structure. In Figs. 9, the calculated spectra for fcc Ni are shown. A similar dependence of the Re σ_{xx} and Im $\omega\sigma_{xy}$ spectrum on the lattice parameter as those for Co is observed.

Tables I and II summarizes the $3d$-band width W_d and its variation ΔW_d, which correspond to the lattice parameter a used in the present computations, together with the atomic volume V and the energy shift of the zero-crossing point of the Im $\omega\sigma_{xy}$ spectrum ΔE for both fcc Co and Ni, respectively. We estimated W_d from the energy difference between W_1^l and X_5 points. W_d varies in an inverse fashion with the lattice parameter. A 5% increase of the lattice parameter result in a 0.88 and a 0.72 eV decrease of W_d for fcc Co and Ni, respectively. It also leads to a 0.4–0.5 eV lower-energy shift in the zero-crossing point of the Im $\omega\sigma_{xy}$ spectrum. The values of $\Delta E = 0.4$–0.5 eV are required to explain the observed differences between the Im $\omega\sigma_{xy}$ spectrum of the 20 and 1000 Å thick fcc Co and Ni films.

V. DISCUSSION

As described in a previous section, we find that the lateral lattice parameters of 20 Å thick films are expanded about 1.4–2.0 % compared with those of thick films. Without any tetragonal distortion normal to the lattice planes, the larger lateral lattice parameter causes a narrowing of the $3d$-band width. Our RHEED experiments cannot provide any information about the perpendicular distances. However, recent low-energy electron-diffraction (LEED) analysis and low-angle x-ray scan for multilayers showed that a few monolayers thick Co(001) film had a contracted interlayer spacing compared with those of thick films.[38–40] On an average, the interlayer spacing of 1.75 Å was reported corresponding to a perpendicular lattice parameter of 3.50 Å. The value is about

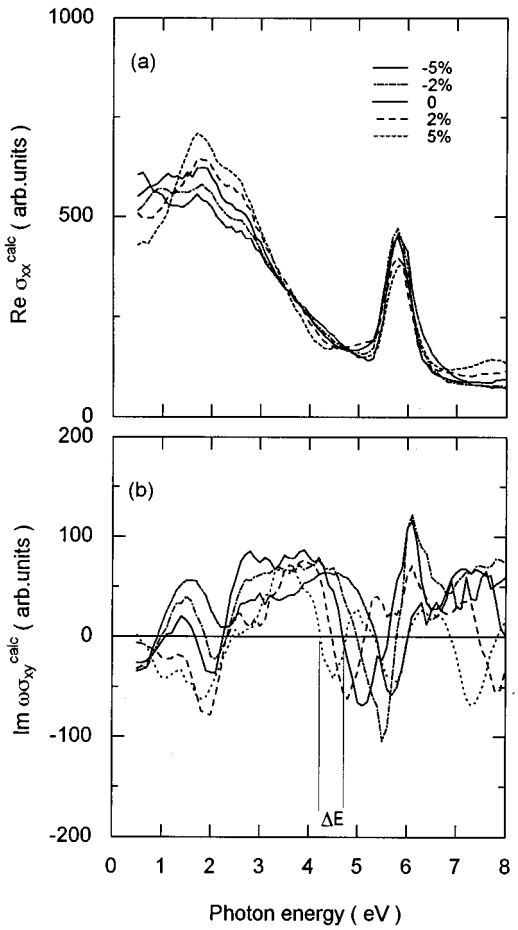

FIG. 9. Calculated conductivity spectra for fcc Ni as a function of the lattice parameter.

2% smaller than that for bulk fcc Co. If we combine the value $c=3.50$ Å with the lateral lattice parameter $a=3.59$ Å, we get a value of 11.21 Å^3/atom for the atomic volume. This value is expanded by about 1.7% compared with that of the bulk fcc Co ($a=3.54$ Å; 11.09 Å/atom). Another LEED analysis reported an interlayer spacing of 1.71 Å for a 10 Å thick Ni/Cu(001) film.[26] In this case, we get a value of 11.02 Å^3/atom which is about 1.1% larger than that for the bulk fcc Ni ($a=3.52$ Å; 10.90 Å/atom). As shown in Table I, if we assume that the 0.88 eV decrease of the $3d$-band width W_d of Co is caused by lattice expansion alone, a 5% increase of the lattice parameter is required. It causes a 16% increase of the atomic volume. This is not only far beyond the experimental estimation but also an unrealistic value, because it requires a large increase of the total energy.[41] That is to say, we cannot explain the observed changes in the Im $\omega\sigma_{xy}$ by means of our calculated difference of bandwidth on the lattice parameter. Our calculations of the electronic structure were restricted only to fcc structure for a infinite specimen. Consequently, the effects such as reduced atomic coordination number in the surface and in the interfacial region with Cu were not considered. We think that these effects play a major roll in the modification of the electronic structure of the ultrathin films. Concerning the surface effect, an *ab initio* calculation presented by Li, Freeman, and Fu[42] is very suggestive. They have calculated the electronic structure of both five- and nine-layer fcc Co slabs and found a $3d$ band narrowing of about 0.5 eV in the surface layer. They, however, mentioned the surface effect was localized mostly inside the surface layer. In the interface with Cu where atomic roughness exists, we should consider a local environment of each Co or Ni atom which is specified by the number of Cu atoms on the nearest-neighbor shell. According to Hamada's investigation[43] in ferromagnetic Ni-Cu alloys, the local density of states of a Ni atom drastically varies with its local environment. It implies that the Cu atoms have an effect on the reduction of the atomic coordination of the Ni atom, since the most of the Cu states sink deeply below the Fermi level. Thus, an interdiffusion of Cu into Co or Ni layers may cause the narrowing of $3d$-band width of the ferromagnet.

In conclusion, we have shown that the shift to lower energies in the high-energy structure of the off-diagonal conductivity spectra of 20 Å thick films is probably caused by the reduction of the $3d$-band width. We have speculated that this reduction in $3d$-band width might be due to the tetragonal compression together with the expansion of the atomic volume due to the lattice mismatch in the interface, and together with the reduced atomic coordination number in the surface and in the interface with Cu.

TABLE I. Lattice parameter dependence of the calculated $3d$-band width and the energy shift of the zero-crossing point of the Im $\omega\sigma_{xy}$ spectrum for fcc Co.

a (Å)	Δa (%)	V (Å^3/atom)	ΔV (%)	W_d (eV)	ΔW_d (eV)	ΔE (eV)
3.36	−5	9.51	−16	6.42	1.22	0.7
3.47	−2	10.44	−6	5.64	0.44	0.3
3.54	0	11.09	0	5.2	0	0
3.61	2	11.77	6	4.81	−0.39	−0.3
3.72	5	12.84	16	4.32	−0.88	−0.5

TABLE II. Lattice parameter dependence of the calculated $3d$-band width and the energy shift of the zero-crossing point of the Im $\omega\sigma_{xy}$ spectrum for fcc Ni.

a (Å)	Δa (%)	V (Å^3/atom)	ΔV (%)	W_d (eV)	ΔW_d (eV)	ΔE (eV)
3.34	−5	9.35	−16	5.59	1.01	0.8
3.45	−2	10.26	−6	4.94	0.36	0.3
3.52	0	10.90	0	4.58	0	0
3.59	2	11.57	6	4.26	−0.32	−0.2
3.70	5	12.62	16	3.86	−0.72	−0.4

ACKNOWLEDGMENTS

The authors would like to thank Dr. Y. Suzuki of the National Institute for Advanced Interdisciplinary Research for useful discussions. This work was supported in part by a Grant-in-Aid for Japanese Junior Scientists from the Ministry of Education, Science, Sports and Culture, and by the New Energy and Industrial Technology Development Organization (NEDO).

*Present address: Advanced Research Laboratory, Toshiba Corporation, Kawasaki 210, Japan
[1] W. B. Zeper, F. J. A. M. Greidanus, P. F. Carcia, and C. R. Fincher, J. Appl. Phys. **65**, 4971 (1989).
[2] S. Hashimoto, A. Maesaka, K. Fujimoto, and K. Bessho, J. Magn. Magn. Mater. **121**, 471 (1993).
[3] W. Geerts, Y. Suzuki, T. Katayama, K. Tanaka, K. Ando, and S. Yoshida, Phys. Rev. B **50**, 12 581 (1994).
[4] T. Suzuki, D. Weller, C.-A. Chang, R. Savoy, T. Huang, B. A. Gurney, and V. Speriosu, Appl. Phys. Lett. **64**, 2736 (1994).
[5] D. Weller, G. R. Harp, R. F. C. Farrow, A. Cebollada, and J. Sticht, Phys. Rev. Lett. **72**, 2097 (1994).
[6] K. Nakajima and T. Miyazaki, *Proceedings of the Magneto-Optical Recording International Symposium '94* [J. Magn. Soc. Jpn. **19**, Suppl. S1, 247 (1994)].
[7] G. S. Krinchik and A. V. Artemiev, Sov. Phys. JETP **26**, 1080 (1968).
[8] J. L. Erskine and E. A. Stern, Phys. Rev. Lett. **30**, 1329 (1973).
[9] K. H. J. Buschow, Ferromagn. Mater. **4**, 493 (1988).
[10] M. Singh, C. S. Wang, and J. Callaway, Phys. Rev. B **11**, 287 (1975).
[11] N. V. Smith, R. Lasser, and S. Chiang, Phys. Rev. B **25**, 793 (1982).
[12] D. K. Misemer, J. Magn. Magn. Mater. **72**, 267 (1988).
[13] S. V. Halilov and Yu A. Uspenski, J. Phys. Condens. Matter **2**, 6137 (1990).
[14] P. M. Oppeneer, J. Sticht, T. Maurer, and J. Kubler, Z. Phys. B **88**, 309 (1992).
[15] T. Gasche, M. S. S. Brooks, and B. Johansson, *Proceedings of the Magneto-Optical Recording International Symposium '94* (Ref. 6), p. 303.
[16] K. Nakajima and T. Miyazaki, J. Appl. Phys. **79**, 4977 (1996).
[17] K. Nakajima and T. Miyazaki, J. Magn. Soc. Jpn. **16**, 580 (1992).
[18] J. F. Dillon, Jr., E. M. Gyorgy, F. Hellman, L. R. Walker, and R. C. Fulton, J. Appl. Phys. **64**, 6098 (1988).
[19] K. Sato, Jpn. J. Appl. Phys. **20**, 2403 (1981); P. Q. J. Nederpel and J. W. D. Martens, Rev. Sci. Instrum. **56**, 687 (1985).
[20] For instance, P. S. Hauge, Surf. Sci. **96**, 108 (1980).
[21] C.-A. Chang, J. Magn. Magn. Mater. **109**, 243 (1992).
[22] J. W. Matthews and J. L. Crawford, Thin Solid Films **5**, 187 (1970).
[23] C. Chappaert and P. Bruno, J. Appl. Phys. **64**, 5736 (1988).
[24] B. Heinrich, J. F. Cochran, M. Kowalewski, J. Kirchner, Z. Celenski, A. S. Arrot, and K. Myrtle, Phys. Rev. B **44**, 9348 (1991).
[25] C. M. Schneider, P. Bressler, P. Schuster, J. Kirchner, J. J. de Miguel, and R. Miranda, Phys. Rev. Lett. **64**, 1059 (1991).
[26] M. T. Johnson, R. Jungblut, P. J. Kelly, and F. J. A. den Broeder, J. Magn. Magn. Mater. **148**, 148 (1995).
[27] S. Z. Wu, G. J. Mankey, F. Huang, and R. F. Willis, J. Appl. Phys. **76**, 6434 (1994).
[28] W. L. O'Brien and B. P. Tonner, Phys. Rev. B **49**, 15 370 (1994).
[29] S. Visinovsky, V. Parizek, M. Nyvlt, P. Kielar, V. Prosser, and R. Krishnan, J. Magn. Magn. Mater. **127**, 135 (1993).
[30] P. B. Johnson and R. W. Cristy, Phys. Rev. B **9**, 5056 (1974).
[31] N. V. Smith and L. F. Mattheiss, Phys. Rev. B **9**, 1341 (1974).
[32] J. C. Slater and G. F. Koster, Phys. Rev. **94**, 1498 (1954).
[33] C. S. Wang and J. Callaway, Phys. Rev. B **9**, 4987 (1974).
[34] E. I. Blout, in *Solid State Physics: Advances in Research and Applications*, edited by F. Seitz and D. Turnbull (Academic, New York, 1962), Vol. 13, p. 305.
[35] P. N. Argyres, Phys. Rev. **97**, 334 (1955).
[36] B. R. Cooper, Phys. Rev. **139**, 1504 (1965).
[37] P. M. Oppeneer, T. Maurer, J. Sticht, and J. Kubler, Phys. Rev. B **45**, 10 924 (1992).
[38] A. Clarke, G. Jennings, R. F. Wills, P. J. Rous, and J. B. Pendry, Surf. Sci. **187**, 327 (1987).
[39] E. Navas, P. Schuster, C. M. Schneider, J. Kirchner, A. Ceballada, C. Ocal. R. Miranda, J. Cerda, and P. de Andres, J. Magn. Magn. Mater. **121**, 65 (1993).
[40] Y. Suzuki (unpublished).
[41] P. M. Marcus and V. L. Moruzzi, Solid State Commun. **55**, 971 (1985).
[42] Chun Li, A. J. Freeman, and C. L. Fu, J. Magn. Magn. Mater. **75**, 53 (1988).
[43] N. Hamada, J. Phys. Soc. Jpn. **50**, 77 (1981).